Vol. 287: 33–43, 2005 | MARINE ECOLOGY PROGRESS SERIES
Mar Ecol Prog Ser | Published February 18

Linking chlorophyll–nutrient dynamics to the Redfield N:C ratio with a model of optimal phytoplankton growth

Markus Pahlow*

Dalhousie University, 1355 Oxford Street, Halifax, B3H 4J1 Nova Scotia, Canada
Bedford Institute of Oceanography, PO Box, 1006 Dartmouth, B2Y 4A2 Nova Scotia, Canada

ABSTRACT: The Redfield N:C ratio is a fundamental quantity in marine biogeochemistry because it is a key determinant of the efficiency of the biological carbon pump, yet no convincing explanations have been put forward for its remarkable constancy over much of the world ocean. Phytoplankton growth models have so far been unable to account for the different relationships between growth rate and N:C ratio under nutrient and light limitation, and have not been able to predict the Redfield N:C ratio. A relatively simple model of coupled chlorophyll and nutrient dynamics is developed from the premise that phytoplankton maximize growth by optimally allocating nutrient and energy resources among competing metabolic requirements for nutrient uptake, light-harvesting, and growth. The model reconciles nutrient and light limitation and appears valid under both balanced and non-balanced growth conditions. The Redfield N:C ratio and its constancy are explained as a result of evolutionary pressure towards maximizing light-limited growth rates in relatively carbon-rich oceanic waters.

KEY WORDS: Light limitation · Nutrient limitation · Phytoplankton growth model · Redfield N:C

Resale or republication not permitted without written consent of the publisher

INTRODUCTION

The Redfield nitrogen:carbon (N:C) ratio is a fundamental biogeochemical quantity used as a major determinant of the efficiency of the biological carbon pump (Volk & Hoffert 1985). It is often associated with the N:C ratio of nutrient-replete phytoplankton, and while strong variations are observed on small spatial and temporal scales, it is remarkably constant on larger scales throughout most of the world ocean (Li et al. 2000, Geider & La Roche 2002). No convincing explanation has been put forward for its value and global constancy, which has been interpreted, however, as indicating that phytoplankton growth rates are usually light-limited in the ocean (Goldman et al. 1979, Tett et al. 1985). Thus, it appears logical that a thorough understanding of light-limited N:C ratios is a prerequisite to understanding the Redfield N:C ratio. While the behavior of phytoplankton N:C ratios under light limitation has been examined experimentally (Laws & Bannister 1980, Falkowski et al. 1985b, Thompson et al. 1989), models used to represent primary production in larger biogeochemical models have only been able to predict nutrient-limited N:C ratios.

Many phytoplankton models have been derived from observations under conditions of balanced growth, i.e. constant chemical composition on a daily timescale. Under these conditions phytoplankton are considered nutrient-limited when growth rate is determined by dilution rate (chemostat), and light-limited when growth rate is controlled by light intensity (turbidostat or semi-continuous culture). Individual nutrient- or light-limited experiments have been modeled quite successfully (Shuter 1979, Laws & Bannister 1980, Laws & Chalup 1990, Baumert 1996, Geider et al. 1998b), but no previous model has been able to reproduce the differential behavior of carbon, nitrogen, and chlorophyll observed under nutrient and light limitation. Transient effects pose additional difficulties for describing non-balanced growth (Flynn 2003). Especially the initial lag phase in batch cultures and with pulsed nutrient supply could only be simulated with the help of specific time lags (Caperon 1969, Cunningham 1984), which are difficult to generalize.

*Address for correspondence: Dartmouth
Email: pahlowm@mar.dfo-mpo.gc.ca

© Inter-Research 2005 · www.int-res.com

Previous phytoplankton models have been constructed from empirically derived formulations of individual processes, such as photosynthesis as a function of irradiance or growth as a function of cellular nutrient content (Platt & Jassby 1976, Droop 1983, Geider et al. 1998b). Theoretical derivations have been given by Aksnes & Egge (1991) for nutrient uptake and by Baumert (1996) for photosynthesis and photoacclimation, but a unifying concept connecting nutrient and chlorophyll dynamics is lacking (Haney & Jackson 1996). Such unifying theory is introduced here in the form of the hypothesis that phytoplankton cells maximize their growth rate by optimally allocating their limited nutrient and energy resources among competing metabolic requirements. This hypothesis is used as an overarching concept to integrate individual cellular functions into a consistent description of algal chlorophyll and nitrogen dynamics.

Phytoplankton models for balanced growth based on optimization theory (Rosen 1967) have been derived previously by Shuter (1979) and Laws & Chalup (1990). These models optimize growth rate by allocating biomass among functional and structural intracellular compartments and maximizing the efficiency of the whole cell. The use of only 1 resource (biomass) necessitates a fixed N:C ratio in the functional compartments, and may be mainly responsible for the inability to simulate light-limited N:C ratios. The use of nitrogen as an additional intracellular resource in the model presented below explicitly recognizes the significant metabolic cost incurred by nitrogen assimilation and the role of nitrogen as an essential constituent of the cell's enzyme apparatus, and allows the extension of algal growth theory towards light-limited N:C ratios.

MODEL

The model uses carbon as the basic unit of both biomass and metabolic energy in the forms of a reductant (NADPH) and ATP. Biomass is thus equivalent to chemical energy and hence all metabolic processes can be considered energy-processing activities in terms of both energy consumed and carbon involved in the reactions. Energy and energy-processing capacity are considered the cell's 2 principal resources necessary for growth.

The following simplifying assumptions facilitate formulating an optimal fractionation of energy and energy-processing capacity: (1) reaction velocity is proportional to enzyme concentration; (2) cellular N is proportional to cellular enzyme; (3) the chloroplast's N:C ratio is the same as that of the whole cell; and (4) production of all organic compounds involves both light and dark reactions. Contrary to common usage, whereby light reactions refer to photochemical reactions directly driven by light energy, the term light reaction here refers to processes actually occurring (for whatever reason) only in the presence of light, whereas dark reactions occur in both light and dark. Energy-processing capacity is defined here as the product of enzyme concentration or fraction and the corresponding energy or biomass turnover rate.

Growth is optimized here via a 3 way partitioning of the cell's energy (or biomass) and nutrient resources: (1) relative amounts of enzymes responsible for light and dark reactions are adjusted in such a way that the whole enzyme apparatus is used most efficiently; (2) newly fixed carbon is divided between the photosynthetic apparatus and the rest of the cell so as to maximize the net energy generation available to the rest of the cell; (3) enzymes are partitioned between energy-generating and energy-processing reactions. Net energy output from the photosynthetic apparatus then drives nitrogen acquisition and processing in an effort to achieve an N:C ratio as close as possible to the N:C ratio maximizing growth rate.

The total enzyme content of a cell can be split into a fraction, f_l, with maximum specific reaction rate μ_l and associated with light reactions; and a fraction, f_d, with maximum specific reaction rate μ_d and associated with dark reactions. Both enzyme fractions are optimally utilized if all energy processed by Fraction f_l can be processed by Fraction f_d and all of f_d is continuously active, which, with Assumptions (1) and (4), is fulfilled by:

$$D\mu_l f_l = \mu_d f_d \quad (1a)$$

$$f_l + f_d = 1 \quad (1b)$$

where D is daylength as a fraction of 24 h. The daytime energy turnover capacity of the cell can then be defined as:

$$\mu^* = \mu_l f_l = \frac{\mu_d}{D + r_D},\ r_D = \frac{\mu_d}{\mu_l} \quad (2)$$

whence the continuous energy-processing capacity is given by $\mu_d f_d = D\mu^*$.

Photosynthesis. Cellular nitrogen as a proxy for enzyme content (Assumption 2) is represented here by the biomass-normalized N quota, or N:C ratio (Q). Q can be partitioned into a fraction ($Q - Q_0$) dedicated to the generation of chemical energy from light, and a fraction (Q_0) processing this chemical energy (Fig. 1). Thus, $Q - Q_0$ is associated with the protein component of the photosynthetic apparatus, consistent with the disproportionate reduction of chloroplast protein under N limitation (Geider et al. 1998a). Owing to Assumption (4) above, both Q_0 and $Q - Q_0$ comprise enzymes responsible for light and dark reactions. Thus, the partitioning between Q_0 and $Q - Q_0$ is assumed to be orthogonal to that between f_l and f_d, i.e. f_l and f_d subdivide both Q_0 and $Q - Q_0$ equally.

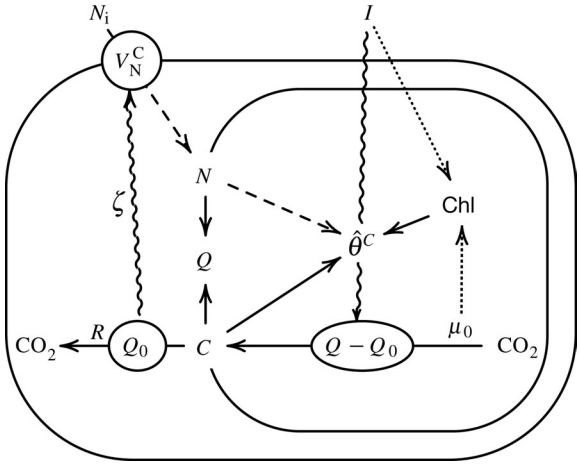

Fig. 1. Major carbon (——), nitrogen (– –), and energy (〰) fluxes and controls (·····) in a phytoplankton cell. Light reactions in chloroplast performed by enzymes associated with $Q - Q_0$ generate energy fueling CO_2 fixation (μ_g). Chlorophyll (chl) is considered a form of carbon. Assimilation of C and N into biomass and chl synthesis determine Q and $\hat{\theta}^C$ as determined by ambient nutrient (N_i) concentration and irradiance I. Dark respiration associated with Q_0 drives biosynthetic processes and nitrate reduction in cytoplasm and determines nutrient uptake at cell surface (V_N^C) via parameter ζ. Definitions of parameters here and in later figures are given in Table 1

With Assumption (3), the chloroplast chlorophyll:carbon (chl:C) ratio ($\hat{\theta}^C$) is defined as:

$$\hat{\theta}^C = \theta^C \frac{Q}{Q - Q_0} \tag{3}$$

where θ^C is the chl:C ratio. $\hat{\theta}^C$ is a better proxy for the amount of pigments associated with the photosynthetic apparatus in the thylakoids than θ^C. The rate of energy generation per unit chlorophyll is then (Baumert 1996):

$$P = \frac{\mu^\star}{\hat{\theta}^C} S_I, \quad S_I = 1 - e^{-\alpha I \frac{\hat{\theta}^C}{\mu^\star}} \tag{4}$$

where α is the chlorophyll-specific light-absorption coefficient, I is irradiance, S_I is the degree of light saturation of the photosynthetic apparatus, and photoinhibition is ignored for simplicity. The gross rate of photosynthetic energy generation in the light or instantaneous gross growth rate follows as:

$$\mu_g = P\theta^C = \mu^\star \frac{Q - Q_0}{Q} S_I \tag{5}$$

The instantaneous growth rate is obtained by subtracting respiration (R):

$$\mu = \mu_g - R \tag{6}$$

If one identifies Q_0 with the subsistence quota, Eqs. (3) to (5) provide a theoretical derivation of Droop's (1983) cell-quota model for nutrient limitation. The photosynthesis–irradiance relationship (S_I) is very similar to that employed by Geider et al. (1998b) except for the daylength-dependence of $\mu^\star$ and that $\hat{\theta}^C/\mu^\star$ depends on $(Q - Q_0)/Q$ rather than being a linear function of Q.

Photoacclimation. Let ξ designate the amount of carbon associated with chlorophyll within the photosynthetic apparatus and representing the biomass comprising the thylakoid membranes as well as the pigments themselves. Then net C fixation can be divided into a fraction ($\mu\xi\hat{\theta}^C$) used for chlorophyll synthesis within the chloroplast, and the remaining carbon $\mu(1 - \xi\hat{\theta}^C)$ available for other compounds. Synthesizing more chlorophyll will increase S_I, and hence P (Eq. 4), but also the fraction $\xi\theta^C$, thereby impeding the ability of the cell to optimize its nutrient uptake rate (see Eq. 17 below). Thus, an optimal allocation of newly fixed C should maximize net output from the photosynthetic apparatus, which is achieved by maximizing the product $S_I(1 - \xi\hat{\theta}^C)$. The following equation describes chlorophyll synthesis emphasizing regulation of θ^C:

$$\frac{1}{\mathrm{chl}} \frac{\mathrm{d[chl]}}{\mathrm{d}t} = \frac{1}{\theta^C} \frac{\mathrm{d}\theta^C}{\mathrm{d}t} + \mu = \frac{\mu}{\xi} \frac{\partial[S_I(1 - \xi\hat{\theta}^C)]}{\partial\hat{\theta}^C} + \mu \tag{7}$$

where [chl] is phytoplankton chlorophyll concentration. If $\hat{\theta}^C$ is treated as a state variable, the steady-state solution of Eq. (7) is independent of Q (Eq. A1: see Appendix 1), i.e. S_I becomes a sole function of irradiance for balanced growth (Eq. 4). Fig. 2 illustrates the behavior of Eq. (7) under different light regimes.

Eq. (7) was derived from the concept of overall growth optimization, rather than some measure of the current condition of the photosynthetic apparatus, such as the fraction of excited photosynthetic units (Baumert 1996) or quantum efficiency (Geider et al. 1998b). Eq. (7) dynamically balances the requirements for energy generation and nutrient acquisition, which is a precondition for getting as close as possible to the optimal N:C ratio for growth. Eq. (7) links chlorophyll production directly to C assimilation (as in Baumert 1996) instead of N assimilation (as in Geider et al. 1998b). Chlorophyll synthesis is connected to nitrogen assimilation indirectly via the relationship between $\hat{\theta}^C$ and θ^C (Eq. 5).

Nitrogen uptake and assimilation. I follow Geider et al. (1998b) in making respiration a function of nitrogen assimilation (a_N^C) and maintenance respiration (R_M):

$$R = \zeta a_N^C + R_M \tag{8}$$

Nitrogen uptake and assimilation are treated separately with respect to the calculation of respiration, because reduction of inorganic N (N_i) and its assimilation into amino acids take place predominantly in the light, while N_i uptake is a potentially continuous pro-

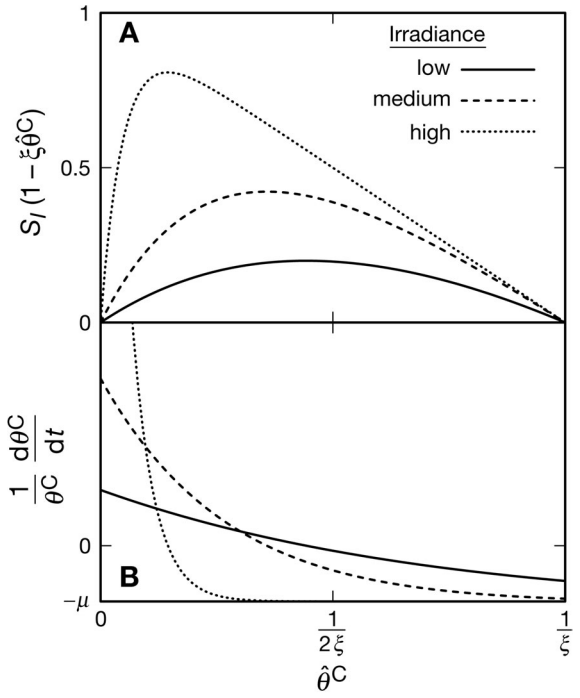

Fig. 2. Dependence of (A) $S_I(1-\xi\hat{\theta}^C)$ and (B) chlorophyll dynamics on $\hat{\theta}^C$ (Eq. 7). Optimal values of $\hat{\theta}^C$ correspond to maxima in (A) and decrease with increasing irradiance. Maximum optimal $\hat{\theta}^C$ (as irradiance approaches 0) is $1/(2\xi)$. Rate of change of $\hat{\theta}^C$ approaches $-\mu$ as $\hat{\theta}^C$ increases beyond its optimal value, such that chlorophyll synthesis can cease completely in actively growing cells

cess (Eppley et al. 1971, Syrett 1981). With respect to Assumption (2) above, it would be more exact to keep track of the difference between total and assimilated intracellular N, but this was not done here for simplicity.

N_i uptake is best described as a function of maximum uptake rate (V^C_{max}) and affinity (A) (Aksnes & Egge 1991):

$$V^C_N = \frac{1}{{V^C_{max}}^{-1} + (A[N_i])^{-1}} \quad (9)$$

where $[N_i]$ is N_i concentration. A major advantage of affinity-based uptake kinetics is that both V^C_{max} and A have equivalents at the cellular level: V^C_{max} is a function of (continuous) N turnover rate, while A depends on the surface area covered by the uptake sites at the cell surface (Aksnes & Egge 1991). Uptake sites are made of protein, for which a certain fraction (f_A) of the available N must be allocated at the expense of the enzyme pool responsible for N turnover within the cell. Due to Assumption (4) above, there is no necessary relationship between f_A and the fractions f_d and f_i. However, the definition of Q_0 suggests that f_A and $1 - f_A$ should be viewed as a subdivision of Q_0. Raising f_A to increase the surface area of uptake sites improves A, but diminishes turnover rate and hence V^C_{max}:

$$A = A_0 f_A \quad (10)$$

$$V^C_{max} = V^C_0 (1 - f_A) \quad (11)$$

where A_0 and V^C_0 are the potential affinity and N_i uptake rate, respectively. Substituting Eqs. (10) & (11) into Eq. (9), setting the derivative of V^C_N with respect to f_A to 0, and solving for f_A maximizes V^C_N:

$$f_A = \frac{1}{\sqrt{\frac{A_0[N_i]}{V^C_0}} + 1} \quad (12)$$

Eqs. (11) & (12) make V^C_{max} a hyperbolic function of N_i concentration, as reported by Kudela & Dugdale (2000). It would appear more appropriate to treat f_A as a time-dependent variable because Eq. (12) describes the long-term behavior of f_A (Kudela & Dugdale 2000), but this was not done here for simplicity.

N assimilation is calculated from V^C_N via the balanced growth approximation:

$$D\mu_g - \zeta V^C_N - R_M = \frac{V^C_N}{Q} - R_M \quad (13)$$

$$\Rightarrow a^C_N = \frac{V^C_N}{D} = \mu^\star \frac{Q - Q_0}{\zeta Q + 1} S_I \quad (14)$$

Eq. (14) calculates N assimilation as if it were restricted to the light period, which may be an oversimplification. Adding nighttime assimilation would have complicated the model significantly, however, and Eq. (14) is only used to estimate the difference between daytime and nighttime respiration (Falkowski et al. 1985a). Substituting a^C_N in Eq. (8) gives a function with a maximum in μ with respect to Q in Eq. (6) at:

$$Q_R = Q_0 + \sqrt{Q_0^2 + \frac{Q_0}{\zeta}} \quad (15)$$

Since ζ units of C must be processed for each unit of N assimilated and the fraction $\xi\theta^C$ of the cell's energy-processing capacity is used for chlorophyll synthesis, the maximum potential N uptake rate is $D\mu^\star(1 - \xi\theta^C)/\zeta$. The net growth rate averaged over 24 h ($\bar{\mu}$) can be approximated by:

$$\bar{\mu} = D\mu_g - D\zeta a^C_N - R_M = D\mu^\star S_I \frac{Q - Q_0}{Q(\zeta Q + 1)} - R_M \quad (16)$$

According to the above theory that the cell tries to maximize its growth rate and given that $\mu^\star$ and S_I are independent of Q, the potential nutrient uptake rate V^C_0 can thus be described by:

$$\frac{V^C_0}{Q} = D\mu^\star \frac{(1 - \xi\theta^C)}{\zeta} \frac{\partial \frac{Q - Q_0}{Q(\zeta Q + 1)}}{\partial Q} \quad (17)$$

where the derivative $\delta \frac{Q - Q_0}{Q(\zeta Q + 1)} / \delta Q$ becomes 0 for $Q = Q_R$.

Model solution and parameterization. Differential equations for C and N complete the model of phytoplankton nitrogen and chlorophyll dynamics:

$$\frac{1}{[C]}\frac{\mathrm{d}[C]}{\mathrm{d}t} = \mu \quad (18)$$

$$\frac{1}{[N]}\frac{\mathrm{d}[N]}{\mathrm{d}t} = \frac{V_N^C}{Q} - R_M \quad (19)$$

where $[C]$ and $[N]$ are phytoplankton C and N concentration, respectively. Calculation of steady-state solutions depends on whether the nutrient concentration or the growth rate is known (Appendix 1).

The model requires specification of 8 parameters: A_0, α, μ_d, Q_0, r_D, R_M, ξ, ζ (Table 1). ζ differs from the other parameters in that it can be estimated from the energy requirement of algal metabolism and the intracellular location of individual reactions involved in nitrogen assimilation. The location is significant because the reductant NADPH and ATP are produced in the chloroplast at a higher ratio than they are consumed (Raven & Beardall 1981). While cyclic photophosphorylation would lower the NADPH:ATP ratio most efficiently, the capacity for this process seems rather limited (Raven 1984a), and if reactions such as nitrate reduction, with a relatively high NADPH:ATP requirement ratio, are accomplished in the chloroplast, they will not incur additional dark respiration.

The total energy requirement of the cell is 2 NADPH and 6 ATP for each C (with ammonium as N_i source) and an additional 4 NADPH for each nitrate assimilated (Raven 1982). Nitrite is reduced to ammonium in the chloroplast (Syrett 1981), such that 2 NADPH and 4 ATP per carbon, 1 ATP and 1 NADPH per nitrogen, and an additional 3 NADPH per nitrate are consumed within the chloroplast (Raven 1982). The remainder of 1.45 ATP per carbon (assuming a C:N ratio of 6.6 and 2.66 mol ATP [mol NAD(P)H]$^{-1}$; Raven 1984b) and, if nitrate reduction takes place in the cytoplasm (Berges 1997), 1 NAD(P)H per nitrate must be generated by dark respiration in the mitochondria. Thus, with 0.188 mol C (mol ATP)$^{-1}$ (Raven 1984b), ζ is 1.8 mol C (mol N)$^{-1}$ for ammonium and 2.3 mol C (mol N)$^{-1}$ for nitrate assimilation. The latter value corresponds well with the slope of dark respiration versus nitrogen assimilation for nitrate-grown *Thalassiosira allenii* (Laws & Wong 1978).

The remaining 7 parameters have been adjusted to give a good fit to the data.

Table 1. Units and definitions of symbols used in text

Symbol	Units	Definition
A	m^3 (mol C d)$^{-1}$	Affinity for inorganic N
A_0	m^3 (mol C d)$^{-1}$	Potential affinity for inorganic N
a_N^C	mol N (mol C d)$^{-1}$	N assimilation rate
α	m^2 g C (µE g chl)$^{-1}$	Light absorption coefficient
C	µmol	Phytoplankton C
Chl	µmol C	Phytoplankton chlorophyll
D	1	Daylength fraction
f_A	1	Protein fraction allocated for affinity
f_d	1	Enzyme fraction for dark reactions
f_l	1	Enzyme fraction for light reactions
I	µE m^{-2} d^{-1}	Irradiance
μ	d^{-1}	Instantaneous growth rate
$\bar{\mu}$	d^{-1}	Average growth rate over 24 h
μ^*	d^{-1}	Daytime energy-turnover capacity
μ_g	d^{-1}	Gross instantaneous growth rate
μ_d	d^{-1}	Dark-specific reaction rate
μ_l	d^{-1}	Light-specific reaction rate
N	µmol	Phytoplankton N
N_i	µmol	Inorganic N
P	g C (g chl d)$^{-1}$	Gross C fixation rate per unit chlorophyll
Q	mol N (mol C)$^{-1}$	Normalized N quota (N:C ratio)
Q_0	mol N (mol C)$^{-1}$	Subsistence N:C ratio
Q_R	mol N (mol C)$^{-1}$	Optimal Q for light-limitation
R	d^{-1}	Dark respiration
r_D	1	Daylength parameter
R_M	d^{-1}	Maintenance respiration
S_I	1	Light saturation
θ^C	g chl (g C)$^{-1}$	Chlorophyll:C ratio
$\hat{\theta}^C$	g chl (g C)$^{-1}$	Chloroplast chlorophyll:C ratio
V_0^C	mol N (mol C d)$^{-1}$	Potential N uptake rate
V_{max}^C	mol N (mol C d)$^{-1}$	Maximum N uptake rate
V_N^C	mol N (mol C d)$^{-1}$	N uptake rate
ξ	g C (g chl)$^{-1}$	C associated with chlorophyll
ζ	mol C (mol N)$^{-1}$	Cost of biosynthesis

RESULTS

Balanced growth

A simulation of the experiment by Laws & Bannister (1980) illustrates the ability of the model to reproduce the difference between nutrient and light limitation. The model is the first to be able to describe all nitrogen- and light-limited data with a single parameter set (Fig. 3, parameter settings in Table 2). Predictions for all 3 modeled compartments of C, N, and chl agree well with the observations. Inorganic nitrogen concentrations in the nutrient- and light-limited experiments span 4 orders of magnitude, demonstrating the model's capability to deal with a wide range of nutrient concentrations. The difference between nitrate and ammonium was represented by different settings for ζ (Table 2).

A notable new feature of the present model is its ability to correctly predict the N:C ratio

Table 2. Parameter settings for results in Figs. 3 to 6. nv: no daylength variation ($\mu^* = \mu_d$)

Symbol	Units	*Thalassiosira fluviatilis*	*Skeletonema costatum*	*Thalassiosira pseudonana*	*Isochrysis galbana*
A_0	m^3 (mmol C $d)^{-1}$	0.97	1.0	0.86	0.01
α	10^{-5} m^2 g C (µE g chl)$^{-1}$	1.8	1.1	7.1	0.9
μ_d	d^{-1}	6.1	3.1	5.1	5.0
Q_0	mol N (mol C)$^{-1}$	0.053	0.043	0.038	0.049
r_D		nv	0.23	nv	nv
R_M	d^{-1}	0.044	0.0	0.20	0.18
ξ	g C (g chl)$^{-1}$	6.4	8.7	11.8	13.2
ζ	mol C (mol N)$^{-1}$	1.8, 2.3[a]	2.3	1.8, 2.3[a]	1.8

[a]Depending on N_i source, see 'Results'

for light-limited growth (Fig. 3A). The decline in N:C ratio with increasing light-limited growth rate results from both a decreasing ratio V_0^C:µ with increasing irradiance and a decreasing ratio V_N^C:V_0^C with increasing V_0^C, for constant nutrient concentration. No explanations have been suggested previously for this relationship between light-limited N:C ratio and irradiance, which has also been observed elsewhere (Falkowski et al. 1985b, Thompson et al. 1989).

Simulation of daylength differences in addition to light and nutrient limitation is demonstrated in Fig. 4. The overall behavior of the algae seems well represented by the model, although some discrepancy exists between predicted and observed curves for individual treatments, primarily at intermediate daylength (Fig. 4B,E). The maximal growth rate is predicted by the sharp bend in each modeled curve in Fig. 4A to C (thick continuous lines) marking the transition from nutrient to light limitation. The predicted chl:N ratio has a maximum at $Q = 2Q_0$ (Eq. 3). Despite the relatively large scatter, such maxima are obvious in all observed curves fairly close to their predicted positions (Fig. 4D to F).

No significant difference between nitrate and ammonium as the limiting nutrient can be discerned in the data and model predictions for nutrient-limited growth in Fig. 3. However, Thompson et al. (1989) found an impact of nitrogen source on light-limited growth. With the above values for ζ, the model accurately reproduces the differences in growth rate and N:C ratio between nitrate and ammonium as N_i source for light limitation (Fig. 5A,C). No significant influence of N_i source on chl:N is predicted by the model and none is visible in the observations (Fig. 5B). Thus, the relative difference in chl:C ratio is very similar to that in the N:C ratio, which accounts for the dependence of growth rate on N_i source.

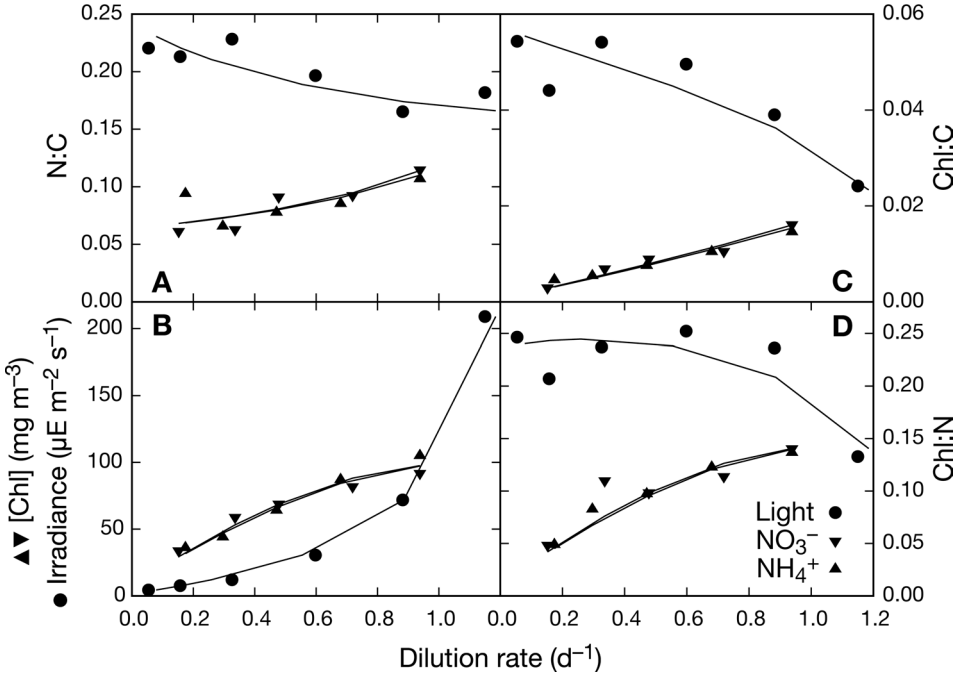

Fig. 3. *Thalassiosira fluviatilis* in light- and nutrient-limited continuous culture. (A) N:C ratio; (B) chlorophyll concentration and irradiance versus dilution rate; (C) chl:C ratio; (D) chl:N ratio. Growth limitation by light (●), nitrate (▼) and ammonium (▲). In (C) model predicts dilution rate for light-limited data. Data from Laws & Bannister (1980), parameter settings in Table 2

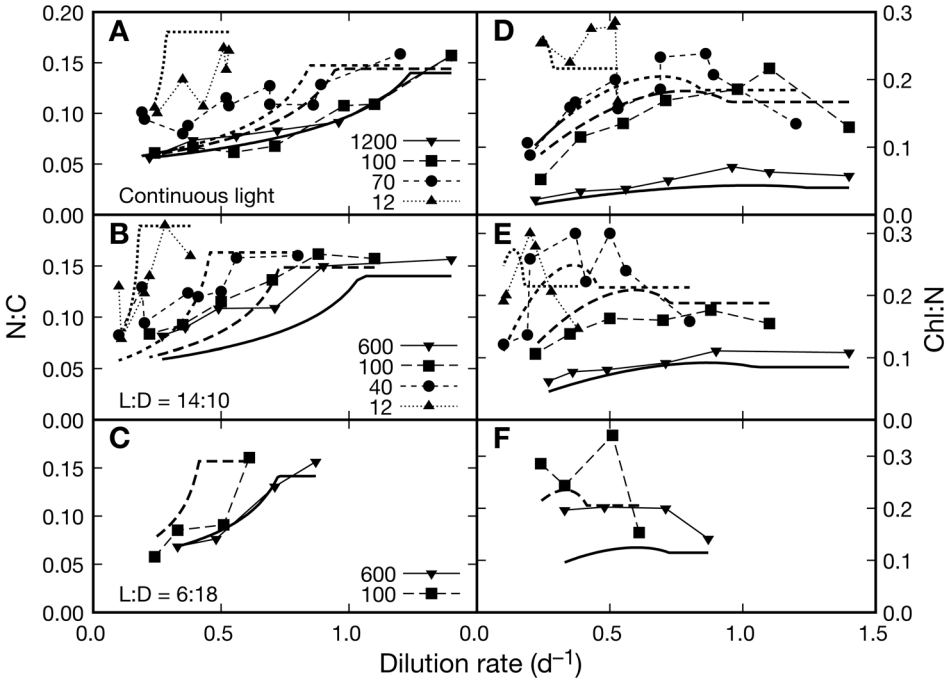

Fig. 4. *Skeletonema costatum* grown under various light intensities and daylengths in continuous culture (L:D, light:dark). (A–C) C:N ratio; (D–F) chl:N ratio. Thick continuous lines: model results; values beside symbols: light levels (μE m^{-2} s^{-1}). Data from Sakshaug et al. (1989), parameter settings in Table 2. Light limitation was assumed for dilution rates when predicted N_i concentration for nutrient-limited growth (Eq. A7) became greater than nutrient concentration in fresh growth medium

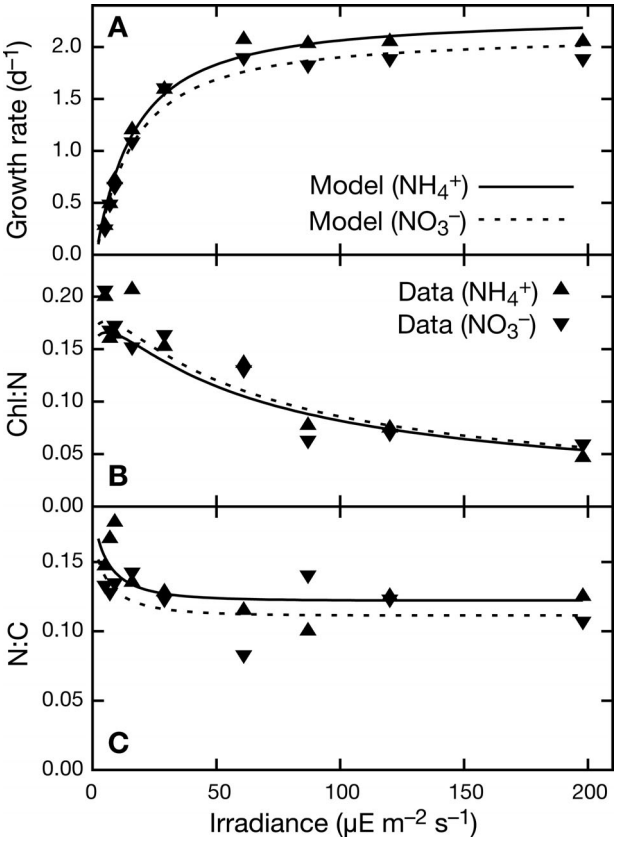

Fig. 5. *Thalassiosira pseudonana* in semi-continuous culture. (A) Growth rate; (B) chl:N ratio; (C) N:C ratio. Simulations for NO_3^- and NH_4^+ were carried out by setting ζ to 2.3 and 1.8 mol C (mol N)$^{-1}$, respectively. Data from Thompson et al. (1989), parameter settings in Table 2

As explained above, the difference in ζ between ammonium and nitrate assimilation depends on the intracellular location of the reduction of nitrate to nitrite, catalyzed by the enzyme nitrate reductase (NR). NR is located partly at the plasmalemma and partly in the cytoplasm in *Thalassiosira* spp. (Jones & Morel 1988), but NR has also been located in chloroplasts of several dinoflagellates and green algae (Fritz et al. 1996). Thus, the dependence of ζ on nitrogen source seen in Fig. 5 may not be universal (Syrett 1981), and the average difference might even be less than the 0.5 mol C (mol N)$^{-1}$ calculated above.

Dynamic growth

The dynamic behavior of the model represents a significant improvement over previous models in that it reproduces the initial lag phase in a batch culture of *Isochrysis galbana* without a specific time lag in the model formulation (Fig. 6). The opposite initial changes in N:C and chl:N (Fig. 6D,E) can only be captured by a model in which chlorophyll synthesis is coupled to C assimilation (Eq. 7) rather than N-assimilation. The model successfully reproduces both the initial response, characterized by rapid N assimilation and the corresponding decrease in chl:N ratio, and the transition towards the stationary phase (Fig. 6).

The initial rapid N_i uptake by the obviously N-starved cells leads to a sharp increase in N:C ratio (Fig. 6D) and consequently in dark respiration (Eqs. 8 & 14). Lack of sufficient chlorophyll causes a shortfall in energy

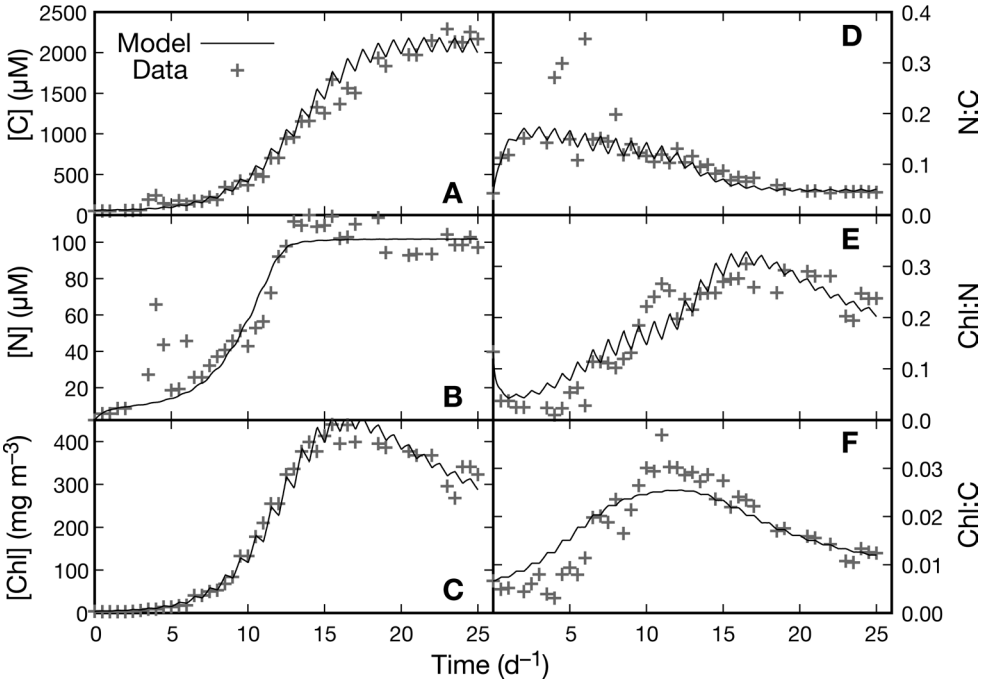

Fig. 6. *Isochrysis galbana* in batch-culture, showing carbon, nitrogen and chlorophyll concentrations and N:C, chl:N and chl:C ratios. Data from Flynn et al. (1994), model setup as in Geider et al. (1998b), except that the simulation was started at the beginning of the experiment; parameter settings in Table 2

supply to cover the higher metabolic cost and delays the photoacclimation process (Eq. 7) by several days. The resulting slow growth rate during this time gives the impression of a suppression of C assimilation by N assimilation in N-deficient cells (Thomas et al. 1976). The decline in chl:N ratio during transition towards the stationary phase is mainly due to the reduction in $(Q - Q_0)/Q_0$ as $\hat{\theta}^C$ and S_I remain almost constant after Day 17 (Fig. 6E).

DISCUSSION

Figs. 3 to 6 show that the model is well suited to simulate phytoplankton growth under a wide range of conditions and to describe a number of hitherto unexplained phenomena, such as the lag phase, the maximum N:C ratio, and the difference between light and nutrient limitation. The relatively small number of parameters needed to accomplish these tasks suggests that the formulation generated by the concept of growth optimization realistically describes individual processes involved in phytoplankton nitrogen and chlorophyll dynamics.

The implied degree of realism combined with its simplicity could make the present model suitable for inclusion within larger ecosystem and biogeochemical models. Transition between nutrient- and light-limited conditions (Fig. 4) and the lag phase (Fig. 6) are important for the timing and extent of phytoplankton bloom events. Handling vast differences in nutrient concentration (Fig. 3) is a prerequisite to reproducing differences between oligotrophic and more eutrophic ocean regions (Harrison et al. 1996). The ability to simulate the light-limited N:C ratio provides a link to the Redfield N:C ratio (see later subsection) and should be of particular interest in biogeochemical applications.

Limitations and potential extensions

The simplicity of the model formulation means that many important processes are not considered. For example, the difference between nitrate and ammonium assimilation can be handled by varying ζ, but the interaction between ammonium and nitrate uptake (Flynn 2003) was not included. Neglecting photoinhibition may be responsible for the slight overestimation of growth rates at high irradiance in Fig. 5A. The relatively high estimate of R_M for *Thalassiosira pseudonana* (Table 2) might indicate release of dissolved organic carbon (Myklestad 2000). The significance of the description of the cost of biosynthesis and of omitting variations in α and diel periodicity has been discussed by Geider et al. (1998b). The time-dependence of f_A is reflected in the rate of change in V^C_{max} (acceleration, Kudela & Dugdale 2000) and might explain part of the lag phase seen in Fig. 6. Differences among parameter settings shown in Table 2 indicate that the model only describes the response of a monospecific phytoplankton population to an experimental treatment but not interspecific differences in this response. The different organization and metabolism of cyanobacteria could invalidate the assumptions made here in calculating respiration in general and ζ in particular, especially for nitrogen-fixing species.

Omission of an explicit treatment of diurnal variablity implies that the model may not be suitable for time scales of days or less. Specifically, the model predicts that photoacclimation after a step-up in irradiance proceeds faster than after a step-down, as do previous models of phytoplankton chlorophyll dynamics (e.g. Baumert 1996, Geider et al. 1998b). While this behavior is opposite to the finding of Cullen & Lewis (1988), it does not appear to compromise the model's performance on longer time scales, as shown in Fig. 6.

It might appear more logical to consider the net energy output of the chloroplasts with respect to the whole cell rather than only to the photosynthetic apparatus, i.e. to maximize $S_I(1-\theta^C)$ rather than $S_I(1-\hat{\theta}^C)$ as was done in Eq. (7). However, this results in a much inferior fit to the data shown here, in particular for the chl:N ratio in Figs. 3D, 4D–F & 5B. My interpretation is that optimizing overall net energy generation by the photosynthetic apparatus, which would introduce a dependence of chl synthesis regulation on N, might not be feasible for an algal cell due to the very different nature and time scale of the variability of inorganic nitrogen supply and irradiance. Eq. (7) allows pigment synthesis to be regulated independently of N, which may simply be more robust than a mechanism which would be slightly advantageous under balanced growth conditions, but might ultimately be far worse most of the time in the patchy and turbulent real ocean. Clearly, more research is needed to resolve this problem.

It may be possible to extend the model to include processes such as photoinhibition, a time dependence of f_A, interaction between nitrate and ammonium uptake, or other limiting nutrients. Application of the concept of optimal resource allocation to nitrogen has been facilitated by the double role of nitrogen in the cellular metabolism as both a major component of enzyme activity and a major contributor to the cost of biosynthesis. Optimal allocation of iron has been applied to colimitation of phytoplankton by light, iron, ammonium and nitrate by Armstrong (1999). Extension of this concept to other processes requires weighing the physiological benefits against the metabolic costs incurred by uptake and assimilation.

The potential gain from a higher overall nitrogen uptake rate may be gauged against the increase in ζ if nitrate is utilized in addition to ammonium. The physiologial roles of phosphorus (P) and iron (Fe) are relatively well known and can be linked to the present parameterization. P is part of many biochemical constituents from DNA to membranes, and is essential for all reactions requiring energy in the form of ATP (Geider & La Roche 2002). In terms of parameters of the present model, this might suggest an influence on the energy-processing capacity, e.g. as represented by μ_d. Growth limitation by Fe, which is a crucial component of the photosynthetic apparatus, seems to affect both the initial slope in the P versus I relationship in Eq. (4) and the maximal carbon fixation rate of the photosynthetic apparatus (Davey & Geider 2001), represented in the present model by α and r_D, respectively.

Link to Redfield N:C ratio

The Redfield N:C ratio is often associated with light limitation in continuous culture. Goldman et al. (1979) turned the argument around and hypothesized that the Redfield N:C ratio implied relatively high phytoplankton growth rates in the surface ocean, whereas Tett et al. (1985) argued that low light intensities could keep growth rates slow. The present model and the data in Figs. 3 to 5 have the highest N:C ratios occurring at the lowest light-limited growth rate, i.e. at the lowest light intensity, and thus support the view of Tett et al. (1985).

One of the most prominent characteristics of the Redfield N:C ratio is its remarkable global constancy throughout the world ocean as opposed, e.g., to conspicuous large-scale variations in N:P ratios (Fanning 1992, Geider & La Roche 2002). Geider & La Roche (2002) estimate 95% confidence limits of 6.8 to 7.8 around a mean C:N ratio of 7.3 for marine particulate matter. In contrast, light-limited N:C ratios exhibit variability in the laboratory, albeit much less than nutrient-limited N:C ratios (Figs. 3 & 4). N:C ratios do vary considerably in the surface ocean on smaller spatial scales, but are smoothed out by mixing on larger scales (Li et al. 2000). Provided the Redfield N:C ratio indeed indicates light limitation in the surface ocean, variations in light-limited N:C ratios observed in the laboratory do not necessarily contradict a globally uniform Redfield N:C ratio on larger scales, as long as the factors determining the light-limited N:C ratio do not form large-scale patterns.

It is apparent from Figs. 3 to 5 that the light-limited N:C ratio is mainly determined by the optimum N:C ratio (Q_R) and light intensity. Q_R in turn is a function only of the 2 parameters Q_0 and ζ. Theoretically derived values for ζ give a reasonable fit to the data presented above, and variations in Q_0 among the different species examined here are relatively minor (Table 2). Subsistence N:C ratios in eukaryotic phytoplankton around 0.03 seem to be typical (Caperon & Meyer 1972, Laws & Bannister 1980, Sakshaug et al. 1989), although substantial interspecific differences ranging from 0.023 to 0.054 have been reported (Caperon & Meyer 1972). Aside from the effect of nitrogen source on ζ, no systematic influence of temperature, light or nutrient regime on these 2 parameters has ever been observed or suggested. Hence, a tight link between the Redfield N:C ratio and Q_R would be consistent with the global constancy of the Redfield N:C ratio.

Although surface irradiance is a function of latitude, the light field experienced by phytoplankton is substantially a function of cloud cover and the depth of the surface mixed-layer, which undergo strong changes on short time scales. In addition, situations of low light intensity, such as the deep chlorophyll maximum or the onset of the spring bloom, are also commonly characterized by a relatively large contribution of nitrate to overall N_i supply (Donald et al. 2001), which could at least partially compensate for the effect of the dim light on the N:C ratio (Fig. 5C). In essence, a globally constant Redfield N:C ratio in the ocean could well be a consequence of evolutionary pressure towards high light-limited phytoplankton growth rates.

Maximizing carbon fixation by trying to achieve an N:C ratio of Q_R obviously requires a sufficient diffusive supply of dissolved inorganic carbon (DIC). This condition is always fulfilled in the ocean, but not in freshwater systems: marine phytoplankton can access the large DIC pool of seawater efficiently with the help of the carbon-concentrating mechanism (Thoms et al. 2001). Restricting the CO_2 supply could potentially affect phytoplankton in either of 2 ways: (1) CO_2 could become the limiting nutrient and increase the N:C ratio analogous to the increase of the N:P ratio under P limitation; (2) CO_2 supply might set the growth rate analogous to the dilution rate in a chemostat. In the latter case, the N:C ratio would be determined only by the growth rate and would be expected to decrease, analogous to the behavior in a P-limited chemostat (Laws & Bannister 1980). Realization of both of these alternatives in different species would be in line with the observations of Burkhardt et al. (1999). The lack of a constant N:C ratio in freshwater systems (Hecky et al. 1993) could then be explained by their much lower DIC concentrations.

Acknowledgements. I wish to thank A. F. Vézina and M. Borek for help in formulating the model and preparing the manuscript. The manuscript benefitted from the input of R. A. Armstrong and 3 anonymous referees. This work was supported by the Department of Fisheries and Oceans' Strategic Science Fund and the Canadian SOLAS Research Network funded by NSERC and the Canadian Foundation for Climate and Atmospheric Sciences.

LITERATURE CITED

Aksnes DL, Egge JK (1991) A theoretical model for nutrient uptake in phytoplankton. Mar Ecol Prog Ser 70:65–72

Armstrong RA (1999) An optimization-based model of iron–light–ammonium colimitation of nitrate uptake and phytoplankton growth. Limnol Oceanogr 44:1436–1446

Baumert H (1996) On the theory of photosynthesis and growth in phytoplankton. Part I: light-limitation and constant temperature. Int Rev Gesamten Hydrobiol 81:109–139

Berges JA (1997) Algal nitrate reductases. Eur J Phycol 32: 3–8

Burkhardt S, Zondervan I, Riebesell U (1999) Effect of CO_2 concentration on C:N:P ratio in marine phytoplankton: a species comparison. Limnol Oceanogr 44:683–690

Caperon J (1969) Time lag in population growth response of *Isochrysis galbana* to a variable nitrate environment. Ecology 50:188–192

Caperon J, Meyer J (1972) Nitrogen-limited growth of marine phytoplankton. I. Changes in population characteristics with steady-state growth rate. Deep-Sea Res 19:601–618

Cullen JJ, Lewis MR (1988) The kinetics of algal photoadaptation in the context of vertical mixing. J Plankton Res 10:1039–1063

Cunningham A (1984) The impulse response of *Chlamydomonas reinhardii* in nitrite-limited chemostat culture. Biotechnol Bioeng 26:1430–1435

Davey M, Geider RJ (2001) Impact of iron limitation on the photosynthetic apparatus of the diatom *Chaetoceros muelleri* Bacillariophyceae. J Phycol 37:987–1000

Donald KM, Joint I, Rees AP, Woodward EMS, Savidge G (2001) Uptake of carbon, nitrogen and phosphorus by phytoplankton along the 20° W meridian in the NE Atlantic between 57.5° N and 37° N. Deep-Sea Res II 48:873–897

Droop MR (1983) 25 years of algal growth kinetics. Bot Mar 26:99–112

Eppley RW, Rogers JN, McCarthy JJ, Sournia A (1971) Light/dark periodicity in nitrogen assimilation of the marine phytoplankters *Skeletonema costatum* and *Coccolithus huxleyi* in N-limited chemostat culture. J Phycol 7:150–154

Falkowski PG, Dubinsky Z, Santostefano G (1985a) Light-enhanced dark respiration in phytoplankton. Verh Int Ver Limnol 22:2830–2833

Falkowski PG, Dubinsky Z, Wyman K (1985b) Growth–irradiance relationships in phytoplankton. Limnol Oceanogr 30: 311–321

Fanning KA (1992) Nutrient provinces in the sea: concentration ratios, reaction rates, and ideal covariation. J Geophys Res 97:5693–5712

Flynn KJ (2003) Modelling multi-nutrient interactions in phytoplankton; balancing simplicity and realism. Prog Oceanogr 56:249–279

Flynn KJ, Davidson K, Leftley JW (1994) Carbon–nitrogen relations at whole-cell and free amino-acid levels during batch growth of *Isochrysis galbana* (Prymnesiophyceae) under conditions of alternating light and dark. Mar Biol 118:229–237

Fritz L, Stringher CG, Colepicolo P (1996) Immunolocalization of nitrate reductase in the marine dinoflagellate *Gonyaulax polyedra* (Pyrrophyta). J Phycol 32:632–637

Geider RJ, La Roche J (2002) Redfield revisited: variability of C:N:P in marine microalgae and its biochemical basis. Eur J Phycol 37:1–17

Geider RJ, Macintyre HL, Graziano LM, McKay RML (1998a) Responses of the photosynthetic apparatus of *Dunaliella tertiolecta* (Chlorophyceae) to nitrogen and phosphorus limitation. Eur J Phycol 33:315–332

Geider R, MacIntyre HL, Kana TM (1998b) A dynamic regulatory model of phytoplanktonic acclimation to light, nutrients, and temperature. Limnol Oceanogr 43:679–694

Goldman JC, McCarthy JJ, Peavey DG (1979) Growth rate influence on the chemical composition of phytoplankton in oceanic waters. Nature 279:210–215

Haney JD, Jackson GA (1996) Modeling phytoplankton growth rates. J Plankton Res 18:63–85

Harrison WG, Harris LR, Irwin BD (1996) The kinetics of nitrogen utilization in the oceanic mixed layer: nitrate and ammonium interactions at nanomolar concentrations.

Limnol Oceanogr 41:16–32
Hecky RE, Campbell P, Hendzel LL (1993) The stoichiometry of carbon, nitrogen, and phosphorus in particulate matter of lakes and oceans. Limnol Oceanogr 38:709–724
Jones GJ, Morel FMM (1988) Plasmalemma redox activity in the diatom *Thalassiosira*. Plant Physiol (Rocky) 87:143–147
Kudela RM, Dugdale RC (2000) Nutrient regulation of phytoplankton productivity in Monterey Bay, California. Deep-Sea Res II 47:1023–1053
Laws EA, Bannister TT (1980) Nutrient and light-limited growth of *Thalassiosira fluviatilis* in continuous culture, with implications for phytoplankton growth in the ocean. Limnol Oceanogr 25:457–473
Laws EA, Chalup MS (1990) A microalgal growth model. Limnol Oceanogr 35:597–608
Laws EA, Wong DCL (1978) Studies of carbon and nitrogen metabolism by three marine phytoplankton species in nitrate-limited continuous culture. J Phycol 14:406–416
Li YH, Karl DM, Winn CD, Mackenzie FT, Gans K (2000) Remineralization ratios in the subtropical North Pacific gyre. Aquat Geochem 6:65–86
Myklestad SM (2000) Dissolved organic carbon from phytoplankton. In: Wangersky PJ (ed) Marine chemistry. Springer, Berlin, p 111–148
Platt T, Jassby AD (1976) The relationship between photosynthesis and light for natural assemblages of coastal marine phytoplankton. J Phycol 12:421–430
Raven JA (1982) The energetics of freshwater algae; energy requirements for biosynthesis and volume regulation. New Phytol 92:1–20
Raven JA (1984a) Light absorption and generation of ATP. In: Energetics and transport in aquatic plants. Liss, New York, p 123–186
Raven JA (1984b) Dark respiration. In: Energetics and transport in aquatic plants. Liss, New York, p 253–317
Raven JA, Beardall J (1981) Respiration and photorespiration. In: Platt T (ed) Physiological bases of phytoplankton ecology. Department of Fisheries and Oceans, Ottawa, p 55–82
Rosen R (1967) Optimality principles in biology. Butterworth, London
Sakshaug E, Andresen K, Kiefer DA (1989) A steady state description of growth and light absorption in the marine planktonic diatom *Skeletonema costatum*. Limnol Oceanogr 34:198–205
Shuter B (1979) A model of physiological adaptation in unicellular algae. J Theor Biol 78:519–552
Syrett PJ (1981) Nitrogen metabolism of microalgae. In: Platt T (ed) Physiological bases of phytoplankton ecology. Department of Fisheries and Oceans, Ottawa, p 182–210
Tett P, Heaney SI, Droop MR (1985) The Redfield ratio and phytoplankton growth rate. J Mar Biol Assoc UK 65: 487–504
Thomas RJ, Hipkin CR, Syrett PJ (1976) The interaction of nitrogen assimilation with photosynthesis in nitrogen deficient cells of *Chlorella*. Planta 133:9–13
Thompson PA, Levasseur ME, Harrison PJ (1989) light-limited growth on ammonium vs. nitrate: what is the advantage for marine phytoplankton? Limnol Oceanogr 34:1014–1024
Thoms S, Pahlow M, Wolf-Gladrow DA (2001) Model of the carbon concentrating mechanism in chloroplasts of eukaryotic algae. J Theor Biol 208:295–313
Volk T, Hoffert MI (1985) Ocean carbon pumps: analysis of relative strengths and efficiencies in ocean-driven atmospheric CO_2 changes. In: Sundquist ET, Broecker WS (eds) The carbon cycle and atmospheric CO_2: natural variations archean to present. American Geophysical Union, Washington, DC, p 99–110

Appendix 1. Steady-state solutions

The balanced-growth solution for $\hat{\theta}^C$ is independent of Q and is obtained by solving $d\theta^C/dt = 0$ in Eq. (7), giving:

$$\frac{\alpha I}{\mu^\star}(1-S_I)\left(1-\xi\hat{\theta}^C\right) = \xi S_I \quad \text{(A1)}$$

Which is most conveniently solved numerically for $\hat{\theta}^C$.

Eq. (9) can be rewritten with the help of Eq. (12) in terms of V_0^C and A_0 as:

$$V_N^C = \frac{A_0[N_i]}{\left(\sqrt{\frac{A_0[N_i]}{V_0^C}}+1\right)^2} \quad \text{(A2)}$$

Light limitation

Under conditions of light limitation, $[N_i]$ is known and balanced growth can be approximated by:

$$D\mu_g - \zeta V_N^C - R_M = \frac{V_N^C}{Q} - R_M \quad \text{(A3)}$$

$$\Leftrightarrow \sqrt{Da_N^C}\left(\frac{1}{\sqrt{A_0[N_i]}}+\frac{1}{\sqrt{V_0^C}}\right) = 1 \quad \text{(using Eqs. 14 \& A2)} \quad \text{(A4)}$$

which can be solved numerically for Q with a_N^C from Eq. (14), V_0^C from Eq. (17), and $\hat{\theta}^C$ from Eq. (A1).

Nutrient limitation

For nutrient limitation, $\bar{\mu}$ is known and balanced growth is approximated by $V_N^C/Q = \bar{\mu} + R_M$, giving, with Eqs. (5) to (8):

$$D\mu_g - \zeta(\bar{\mu} + R_M)Q = \bar{\mu} + R_M \quad \text{(A5)}$$

which is a quadratic function of Q and is solved by:

$$Q = \frac{1}{2\zeta}\left(\frac{D\mu^\star S_I}{\bar{\mu}+R_M}-1\right) - \sqrt{\frac{1}{4\zeta^2}\left(\frac{D\mu^\star S_I}{\bar{\mu}+R_M}-1\right)^2 - \frac{D\mu^\star Q_0 S_I}{\zeta(\bar{\mu}+R_M)}} \quad \text{(A6)}$$

V_0^C can be calculated from Q and $\hat{\theta}^C$, and with Eq. (A2) one obtains $[N_i]$ as:

$$[N_i] = \frac{V_0^C}{A_0\left(\sqrt{\frac{V_0^C}{V_N^C}}-1\right)^2} \quad \text{(A7)}$$

Editorial responsibility: Otto Kinne (Editor-in-Chief), Oldendorf/Luhe, Germany

Submitted: November 19, 2003; Accepted: July 22, 2004
Proofs received from author(s): February 9, 2005